International Journal of Biological Macromolecules 274 (2024) 133310

Contents lists available at ScienceDirect

International Journal of Biological Macromolecules

journal homepage: www.elsevier.com/locate/ijbiomac

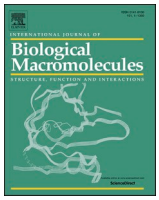

Multiscale assessment of artificial aging treatment of polysaccharides from tonewood species

Mariana Domnica Stanciu [a,*], Horatiu Draghicescu Teodorescu [a], Sorin Vlase [a], Mircea Mihalcica [a], Mihaela Cosnită [b], Adriana Savin [a,c]

[a] Faculty of Mechanical Engineering,Transilvania University of Brasov, 29 Eroilor, 500036, Brasov, Romania
[b] Department of Product Design Mechatronics and Environment, Transilvania University of Brasov, 29 Eroilor, 500036, Brasov, Romania
[c] Institute of Research and Development for Technical Physics, B-dul Mangeron 47, 700050, Iasi, Romania

ARTICLE INFO

Keywords:
Aging
Acoustic
Mechanical properties
Photo-degradation
Crystallinity

ABSTRACT

In the acoustics of musical instruments with a resonator body, the aging of the wood leads to the improvement of the acoustic properties due to increasing the crystallinity of wood. This phenomenon could be explained by the fact that wood is a complex product based on three-dimensional polymer chains of carbohydrates, its aging being closely related to covalent cross-linking and scission of polymer chains. The aim of this study was to evaluate at a multiscale the changes produced artificial aging of tone wood by measuring the acoustic, mechanical and chemical parameters. The spruce and maple wood samples were investigated before and after exposure to ultraviolet (UV) radiation, through the tensile test, the time-of-flight method (TOF), the analysis of the wood color and the determination of the chemical fingerprint through Fourier transform infrared spectroscopy (FTIR) and X-ray diffraction (XRD). The obtained results showed that the effects of artificial aging are manifested at the chemical level where the crystallinity increases up to the acoustic level, depending on the wood species and their quality class. These results are relevant for musical instrument manufacturers to find treatments that lead to superior acoustic properties.

1. Introduction

In the acoustics of musical instruments with a resonator body, it has been assumed that the aging of wood leads to improved acoustic properties. To understand how wood aging contributes to the acoustic qualities of musical instruments, it is essential to analyze detailed and accurate information about the architecture and properties of the resonance wood at different scales [1–3]. The improvement of the acoustic quality of the soundboard through aging starts from the chemical level, by increasing the degree of crystallinity of the cellulose and decreasing the content of amorphous carbohydrates. Analyzing the phenomenon of artificial aging from the macroscale to the nanoscale, it can be considered that the chemical changes produced by artificial aging are manifested by breaking the covalent bonds in the organic compounds of wood, reducing the mass, increasing the stability to humidity variations, and decreasing the lignin content. Even if the chemical changes are not quantitatively at the mechanical/elastic level, nevertheless, at the acoustic level they increase the sound propagation speed. The aging of wood, both through photo-degradation processes and through thermal oxidation, produces changes in the structure of the wood, visible on X-ray radiographs through the difference in the density of the woody compared to that of unaged wood [3–6]. From the point of view of the chemical architecture of wood, it is a complex natural carbohydrate product based on three-dimensional polymer chains of carbohydrates, namely cellulose, hemicellulose and lignin, with minor amounts of extractives and inorganic compounds. In the case of wood for musical instruments, i.e. spruce (*Picea abies Karst. L.*) and maple (*Acer pseudoplatanus L.*), cellulose is found in a proportion of approximately 50.69–50.90 %, being a linear homopolysaccharide, composed of β-D-glucopyranos units, with β-1,4-glycosides covalent bonds, having the role of strengthening the cell walls (Fig. 1a) [7–9]. According to [7–12], hemicelluloses are amorphous polymers, acting as binders in cell walls and ensuring their flexibility. Hemicelluloses have also been found to be essential for the formation of the cellulose microfibril structure during the deposition of cellulose in the cell wall. Hemicelluloses represent a large group of branched heteropolymers, composed of several

* Corresponding author.
E-mail addresses: mariana.stanciu@unitbv.ro (M.D. Stanciu), draghicescu.teodorescu@unitbv.ro (H.D. Teodorescu), svlase@unitbv.ro (S. Vlase), mihalcica.mircea@unitbv.ro (M. Mihalcica), mihaela.cosnita@unitbv.ro (M. Cosnită), asavin@phys-iasi.ro (A. Savin).

https://doi.org/10.1016/j.ijbiomac.2024.133310
Received 30 October 2023; Received in revised form 23 May 2024; Accepted 12 June 2024
Available online 21 June 2024

monomeric units, of which, studies have shown that in softwood such as spruce, xyloglucans have a structural role in the primary cell walls forming, together with cellulose, a load-bearing network that prevents cell breakage under mechanical stress. Fig. 1b shows the structure of xyloglucans. Lignin constitutes a group of branched aromatic biopolymers, being an amorphous carbohydrate, made up of hydroxyphenyl propane units, in a three-dimensional structure. Studies have shown that the main compounds of native lignin are the monolignols known as p-cumaryl alcohol, coniferyl alcohol and sinapyl alcohol (Fig. 1c). Lignin is predominantly found in the secondary cell wall, ensuring the compression resistance of the fibers but also a hydrophobic surface of the fibers, necessary for the transport of water [11–13]. The chemical structure of wood is presented in numerous studies, with details of the chemical compounds and their location in the architecture of the cellular walls of the wood, in both spruce and maple wood.

Cellulose, hemicellulose and lignin chains are found in different proportions and the way the cell walls are formed depends on the genetic information of the wood species. Thus, in spruce wood, the cells with the role of resistance and water transport are the tracheids, and in maple wood, the axial system is made up of fibers and vessels. In musical instruments, in the dry state of the wood, these formations are responsible for the transmission of sounds and vibrations in the longitudinal direction. The effect of wood aging on physical and mechanical properties has been studied, but the literature is quite poor in terms of studies on light photodegradation and thermal oxidation treatments in order to increase the acoustic performance of wood. The aging of the wood can be visually observed by the change in the color of the wood, the color change being large at the beginning of the aging, after which it decreases over time.

According to [14–16], artificial aging methods, such as the lightfastness test with a UVA 351 lamp or heat treatment, have proven to be adequate to simulate color changes due to natural aging. On the other hand, aging by applying a thermal oxidation process leads to the degradation of hemicelluloses, an effect reported by many authors [17–19]. Simultaneous exposure to UV radiation and mild thermal treatment produces color changes and changes in mechanical and durability properties [19–21]. As the hydroxyl content of hemicelluloses decreases, the wood becomes less hydrophilic, resulting in lower equilibrium moisture content (EMC) and better dimensional stability [3,22–24]. This was explained by [8] by the fact that lignin is associated with hemicelluloses, so that lignin carbohydrate complexes are formed, which are resistant to hydrolysis. The weight loss observed during heat treatment by [3,19], is considered also caused by the degradation of hemicelluloses. [25] highlights the fact that artificial aging can change (usually increase) the specific modulus (specific dy-namic Young's modulus) E'/ρ of wood without changing the value of the damping (tan δ). Thus, to increase the specific dynamic Young's modulus, the dry mass loss should be a maximum of 2–3 % by applying a heat treatment at 100 °C and 63 % RH for 30 days, which could lead to wood characteristics corresponding to 500 years of aging. Analyzing the mechanical behavior of modern and aged hinoki wood in the radial (R) and longitudinal (L) directions, [25] found that the difference in behavior between the L and R directions can be explained by the different structural organization of the wood fibers, the post-linear (?) being influenced by the age of the wood.

Thus, the aged wood was brittle, results that correlate with chemical analyzes and thermo-mechanical tests performed in parallel, showing a decrease in hemicellulose content, as well as an increase in lignin crosslinking [25]. Studying the vibrational properties of aged wood (approx. 300 years) compared to those of new wood (8 years old), [26] observed that the wood presented a higher longitudinal and transverse stiffness, a higher speed of sound in the longitudinal direction and a lower damping in the longitudinal direction than the current wood. There are still many controversies concerning the effect of aging on elastic, acoustic and chemical properties. Contrary to the results highlighted by [26], the studies [27–28] show that there are no significant differences from a chemical point of view, between the wood of the old Cremonese violins and the new wood.

Since there are so many controversies related to the effect of artificial aging of wood on its acoustic properties, the main objective of the present paper was to investigate the effect of artificial aging on the physical, elastic, acoustic and chemical properties of the wood to be used for musical instruments. The novelty of the study consists in the multiscale evaluation of the chemical, mechanical and acoustic changes produced by the artificial aging of the current resonance wood in relation to the anatomical structure of the tonewood. Exposing the wood to UV radiation that penetrates the surface of the wood with a maximum depth of 2.5 mm, thickness close to the thickness of the violin boards [29] can be a method to improve the acoustic performance of tone wood, before the final manufacture of the violin.

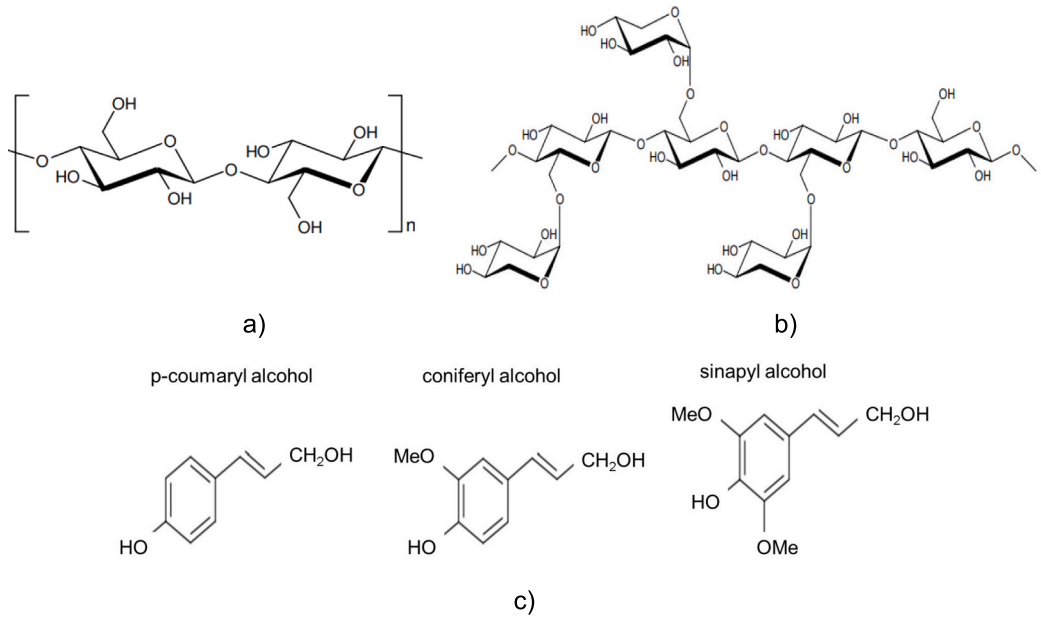

Fig. 1. The main structural polymers from wood: a) β-D-glucopyranose unit from cellulose chain; b) the structure of xyloglucans (hemicellulose); c) the main compounds of native lignin.

2. Materials and methods

2.1. Sample preparation

The wood samples were made of two wood species used for the construction of violins: spruce (*Picea abies (L), Karst*) and maple (*Acer pseudoplatanus, L*). Two sets of samples were prepared: one as control, and the other to be aged. The wood samples were provided by a musical instrument factory. The set of control samples was tensile tested, and the other samples were exposed to artificial aging for 1000 h. After exposure, the samples were investigated for the determination of mass, color and chemical composition, as well as for the comparative processing of the results with the initial data and those of the control samples. Fig. 2 shows the shape and dimensions used both for the tensile test and the velocity of sound measurement (TOF method). The samples were extracted from boards dried naturally for 3 years and mechanically processed under identical conditions. Then, the boards were conditioned to reach a moisture content of 6–8 %. Within each set of samples there were four categories of samples: those from spruce wood, anatomical class A, coded Spruce A, respectively anatomical class D, coded Spruce D, as well as those from maple wood, anatomical class A, coded Maple A, respectively anatomical class D, coded Maple D, according to the description of these categories indicated in previous studies [30–31]. The samples were prepared according to the SR EN 408:2004 standard, obtaining dog-bone type samples, specific to the tensile test (Fig. 2) and samples for the ultrasonic test (US) based on time of flight method (TOF) [32–35]. Table 1 shows the mean values of physical characteristics and sample sizes.

2.2. Methods

2.2.1. Artificial aging of wood

The wood samples were introduced into a photocatalytic reactor being exposed to the ultra-violet (UV) radiation produced by the 3 UV tubes (Philips, TL-D BLB 18 W/108) and 4 VIS light tubes (Philips, TL-D Super 80 18 W/ 865), for a period of 1000 h. The radiation emitted by the UV tubes had wavelengths between 340 and 400 nm, with wavelength λ_{max} (emission) = 365 nm, and the average value of UV radiation measured with a Delta-T pyranometer, type BF3 was 3 W/ m^2 [32,36,37]. Periodically, the samples were controlled, rotated so that there was a uniform exposure on all surfaces. The distance between the samples and the lamps inside the reactor during irradiation was 20 cm, and the temperature inside the irradiation chamber was 50 °C.

2.2.2. Tensile test

To evaluate the changes produced by artificial aging from the mechanical point of view, the elastic characteristics of the wood samples were subjected to the static tensile test also presented in previous works [38–39]. The tests were carried out on the LS100 Lloyd's Instrument universal testing machine belonging to the Mechanical Engineering Department of Transilvania University in Brașov. The samples were loaded at a constant rate of 1 mm/min until failure. Elongation was measured simultaneously with loading using the extension device. Nexygen Plus software was used for data acquisition. Following the tensile tests, the stress-strain curves, the strain (ε), the longitudinal elastic modulus (denoted $E_{L,static}$), the specific modulus ($E_{L,static}/\rho$), the tensile stress (σ), and the stiffness of each category of samples (S), were determined before and after aging.

2.2.3. Determination of sound velocity in wood based on time of flight method (TOF)

The measurement of the velocity of sound propagation in wood in the longitudinal direction (denoted V_L) was carried out using a portable ultrasound device, LUCCHIMETTER, Cremona Italy. The samples, on which the US measurements were performed, were obtained from the same material as the samples used for the tensile test and exposed to the same aging conditions. The determination of sound velocity is based on the time of flight method, which measures the travel time of the wave between two sensors that are inserted into the sample [30,35,40–42]. Delaying the signal over a known distance between the transmitter and the receiver of the US equipment allows the stress wave speed to be calculated. The measurements were carried out under laboratory

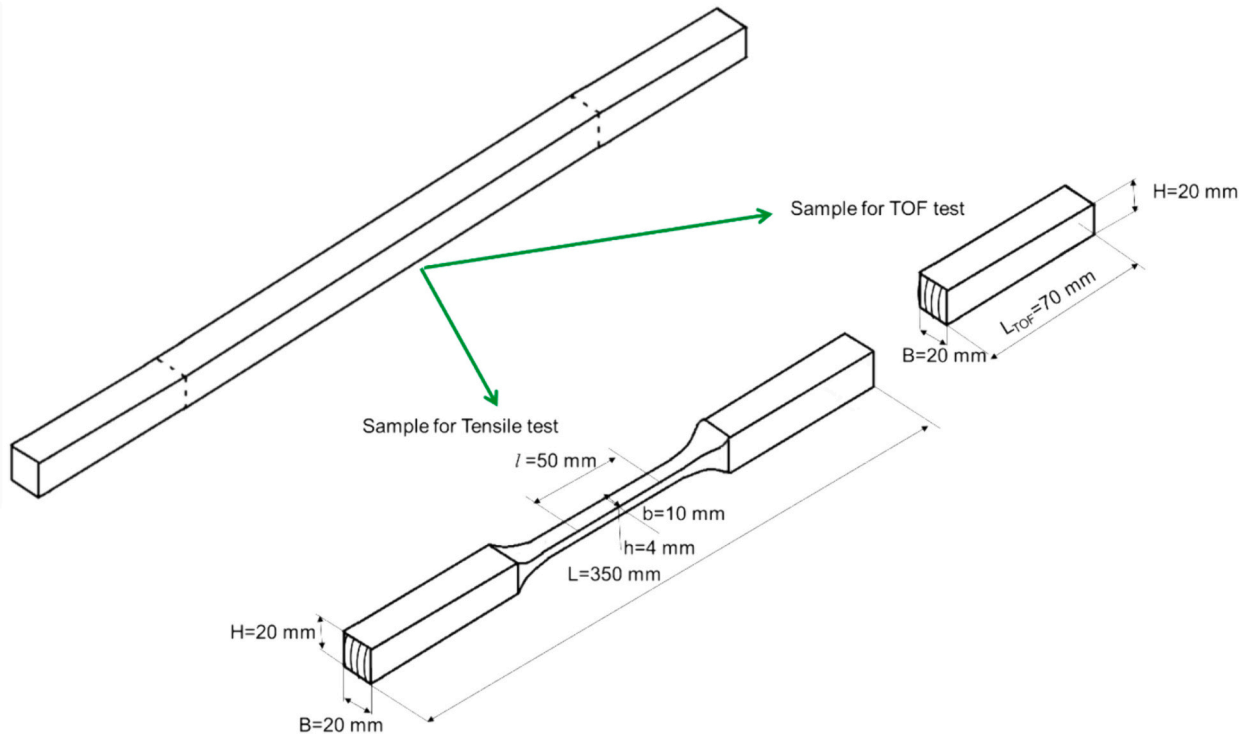

Fig. 2. The geometry of the samples prepared for the experimental investigations.

Table 1
Mean values and standard deviation of the physical characteristics of the tested samples.

Type of samples	Tensile test				TOF test			
	MC (%)	Width b (mm)	Thickness h (mm)	Gauge length *l* (mm)	Length L_{TOF}	Mass (g)	Density (g/cm^3)	No of samples
Spruce A	6.50 (0.8)	9.99 (0.11)	3.98 (0.43)	50	70	11.729 (0.298)	0.397 13)	12
Spruce D	7.01 (0.5)	10.03 (0.10)	4.43 (0.33)	50	70	13.255 (0.900)	0.447 (24)	12
Maple A	7.26 (0.6)	10.09 (0.08)	3.97 (0.14)	50	70	18.683 (0.840)	0.627 (31)	12
Maple D	6.96 (0.5)	10.40 (0.29)	4.23 (0.23)	50	70	17.485 (1.271)	0.577 (38)	12

conditions (at a temperature of 20 ± 4 °C and a humidity of 60 ± 5 %).

Wood density (ρ) of each sample was also determined based on the ratio of mass to volume of the samples measured at each stage of the experiment (before and after UV exposure). First, the dynamic modulus of elasticity (denoted $E_{L,dyn}$) was calculated as a function of ultrasonic velocity (V_L) and density, according to eq. (1) [30,31,35,40–42].

$$E_{L,dyn} = {V_L}^2 * \rho \quad (1)$$

Taking into account the existence of an incremental velocity that develops in small samples, it is necessary to eliminate the effect of the rapid incremental propagation velocity and to take into account the slowest speed of the developing plane wave [33,35,43]. Thus, for calculating the longitudinal modulus of elasticity, [33,35,43] propose the introduction of a correction factor *k* in order to obtain the correct data from the TOF instruments, eq. (1) becoming eq. (2):

$$E^k_{L,dyn} = \left(\frac{V_L}{k}\right)^2 * \rho \quad (2)$$

According to [33,35,43], for an orthotropic medium such as wood, the Kelvin-Christoffel equation gives *k* which is calculated as a function of the Poisson's ratio of the wood (see eq. 3):

$$k = \sqrt{\frac{1 - \upsilon_{RT}\upsilon_{TR}}{1 - \upsilon_{RT}\upsilon_{TR} - \alpha}} \quad (3)$$

where α is:

$$\alpha = 2\upsilon_{RL}\upsilon_{TR}\upsilon_{LT} + \upsilon_{TL}\upsilon_{LT} + \upsilon_{RL}\upsilon_{LR} \quad (4)$$

where υ_{RL}, υ_{LR}, υ_{RT}, υ_{TR}, υ_{TL}, υ_{LT} are the Poisson's ratios of wood.

In this study, based on the experimental values obtained by the tensile test $(E_{L,static})$ and the measurement of the sound propagation speed in the longitudinal direction, the authors calculated the value of the correction factor *k* for spruce and maple samples, before and after artificial aging for 1000 h, using eq. (5):

$$k = V_L\sqrt{\frac{\rho}{E_{L,static}}} \quad (5)$$

Mean values (MV) and standard deviation (SD) of the measured parameters were recorded before and during temperature and UV exposure. The measurements were performed at a temperature of 24 °C and a humidity of 65 %.

2.2.4. Color modification

According to the procedures presented in previous studies [32,37,44], the change in wood color denoted ΔE^* induced by UV and mild heating upon long-term exposure, was calculated based on eq. (6). Color parameters such as lightness L*, redness a*, and yellowness b* were determined experimentally before and after artificial aging, using the Konica Minolta CR-400 chromometer.

$$\Delta E^* = \sqrt{(\Delta L^*)^2 + (\Delta a^*)^2 + (\Delta b^*)^2}, \quad (6)$$

where ΔL^* – the lightness difference between lightness after 1000 h UV exposure ($L^*_{UV1000h}$) and initial lightness (L^*_0); Δa^* – redness difference between redness after 1000 h UV exposure ($a^*_{UV1000h}$) and initial redness (a^*_0) and Δb^* – yellowness difference between yellowness after 1000 h UV exposure ($b^*_{UV1000h}$) and initial yellowness (b^*_0) of wood samples.

The intensity of color or chroma (denoted C^*) is calculated based on eq. (7) [45]:

$$C^* = \sqrt{a^{*2} + b^{*2}}, \quad (7)$$

2.2.5. Fourier transforms infrared spectroscopy (FTIR)

The chemical changes produced by UV and thermal exposure were investigated using a FTIR spectrometer (VERTEX70, Bruker, Ettlingen, Germany) with ATR (Attenuated Total Reflectance) module. The spectra were recorded in the range 4500–500 cm^{-1}, with a resolution of 4 cm^{-1} and 16 scans per sample. Recorded spectra were further processed for baseline correction and smoothing, and average spectra were calculated for each sample category before and after aging using OPUS software (version 7.2, Bruker, Ettlingen, Germany). The working method was adopted according to [32,46,47].

2.2.6. X-ray diffraction (XRD)

Crystallinity data were collected in the 2θ angle range between 10° and 80° in fixed time mode, with a step interval of 0.01° to 25°, using a Bruker Advanced D8 diffractometer (CuKα1 radiation, with a wavelength of 1.5406 Å, at 40 kV and 20 mA) [9].

3. Results and discussion

3.1. Mechanical and acoustic properties modification due to aging

3.1.1. Mechanical properties from tensile test

The stress-strain curves for the spruce and maple wood samples from the two anatomical quality classes, A and D, before and after artificial aging are shown in Fig. 3. It can be seen, as a general trend, that the aged spruce samples appeared stiffer (with higher E) and stronger (higher σ) than before exposure. Similar observations were reported for hinoki wood [25]. The differences in the stress-strain curves are smaller in the case of maple wood samples (maple is a deciduous wood with anatomical characteristics different from those of softwood). The $E_{L,static}$ values for aged spruce wood are slightly higher than those for spruce wood samples before 1000 h of UV exposure, by 2.6 % (class A) and 9,3 % (class D). In the case of maple wood samples, a slight increase in $E_{L,static}$ can be observed by 1.38 % for class D, after aging. Class A maple samples showed a slightly decrease in $E_{L,static}$ after 1000 h of UV exposure (3 %). The artificial aging process led to an increase in the stiffness of the samples as a result of the degradation of the main chemical compounds

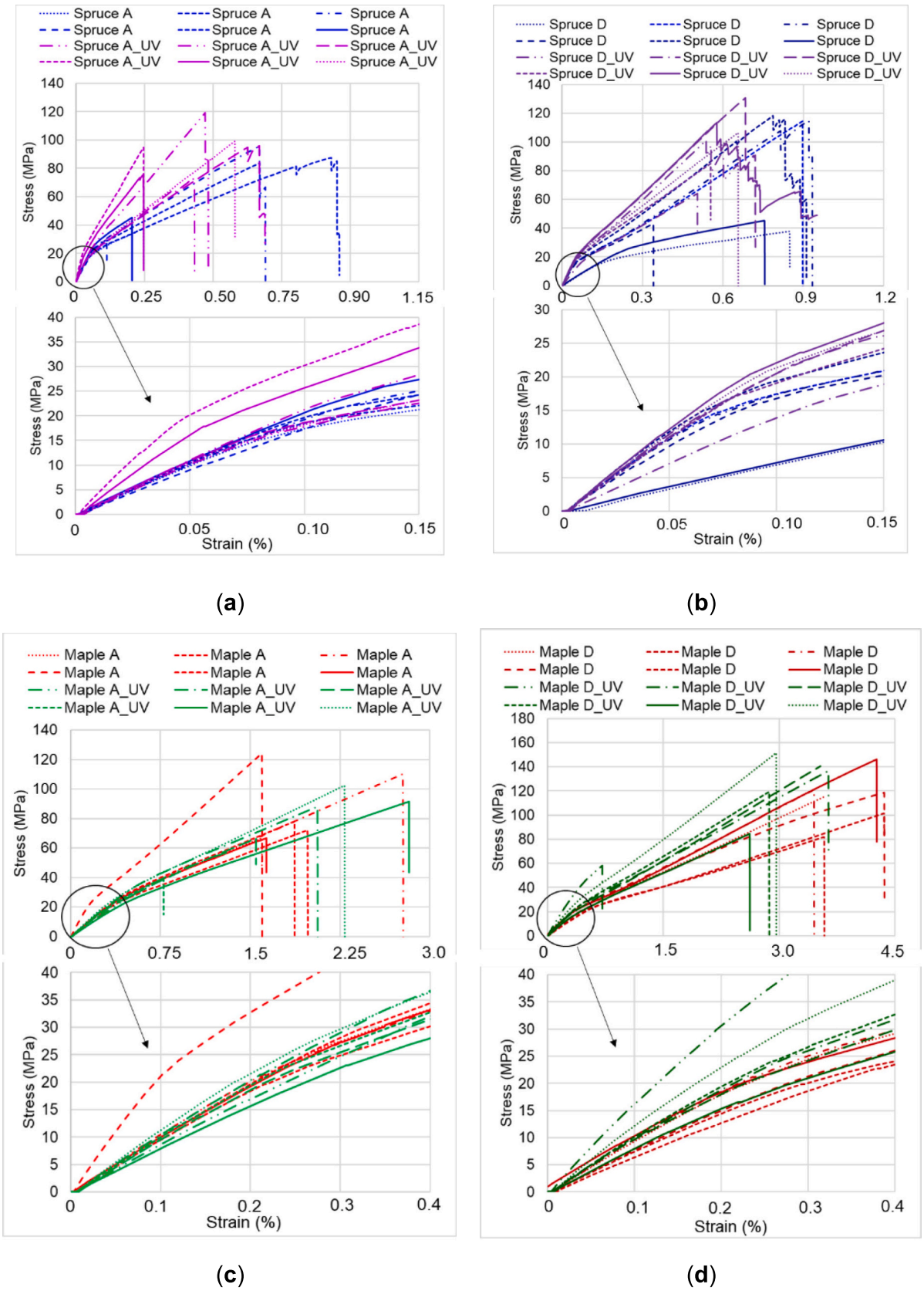

Fig. 3. The stress-strain curves: (**a**) Spruce wood sample class A; (**b**) Spruce wood sample class D; (**c**) Maple wood sample class A; (**d**) Maple wood sample class D.

of the wood.

The way wood breaks is closely related to the orientation of the anatomical elements in relation to the stress axis. According to [40,41], the initiation of tensile failure occurs either inside the cell wall where its layers are subjected to shear and, subsequently, irreversible elongation absorbs the energy without loss of strength [48–49], or between cells, when they have thin walls [50–52]. Fig. 4 shows the tensile failure of the samples, in the case of spruce wood, there are visible differences between the control samples and those subjected to artificial aging for 1000 h. The failure pattern of spruce before UV exposure is chip type, while in the aged spruce samples the mode is pure tension failure.

Fig. 5 shows the regression curves between the static modulus of elasticity and density for the two categories of wood species analyzed (spruce and maple). Due to the anatomical characteristics of maple, the regression curves differ before and after photo-degradation compared to spruce wood. From Fig. 6a it can be seen that only the unaged D spruce wood samples show a regression model that explains 66 % of the stiffness variability with respect to the specific modulus. For maple wood, the R2 value greater than 0.6, as in the case of Maple A, Maple A_UV and Maple D samples, indicates a higher variability explained by the regression model (Fig. 6b).

3.1.2. Acoustic and elastic properties from TOF test

Fig. 7 a,b shows the density stratification of the spruce and maple wood samples, before and after aging. It can be seen that the aging treatments are different depending on the wood species: the spruce wood samples do not undergo considerable changes in density, while, in the case of the maple wood samples, those of class A register a decrease in density with approx. 3 %. On the other hand, UV exposure for 1000 h led to an increase in the speed of sound propagation in spruce wood (by 4.7 % for Spruce A and 5.9 % for Spruce D), compared to maple wood samples, where the propagation speed increased by 2 % for Maple A (Fig. 7c), while the Maple D samples did not show any increase (Fig. 7d).

Table 2 contains the average values of the main mechanical and acoustic properties determined. In Table 2, the correction factors k_L for each sample category vary according to the species and the effect of different photodegradation on the material structure and implicitly by the different values of Poisson's ratio, as highlighted in [24,43].

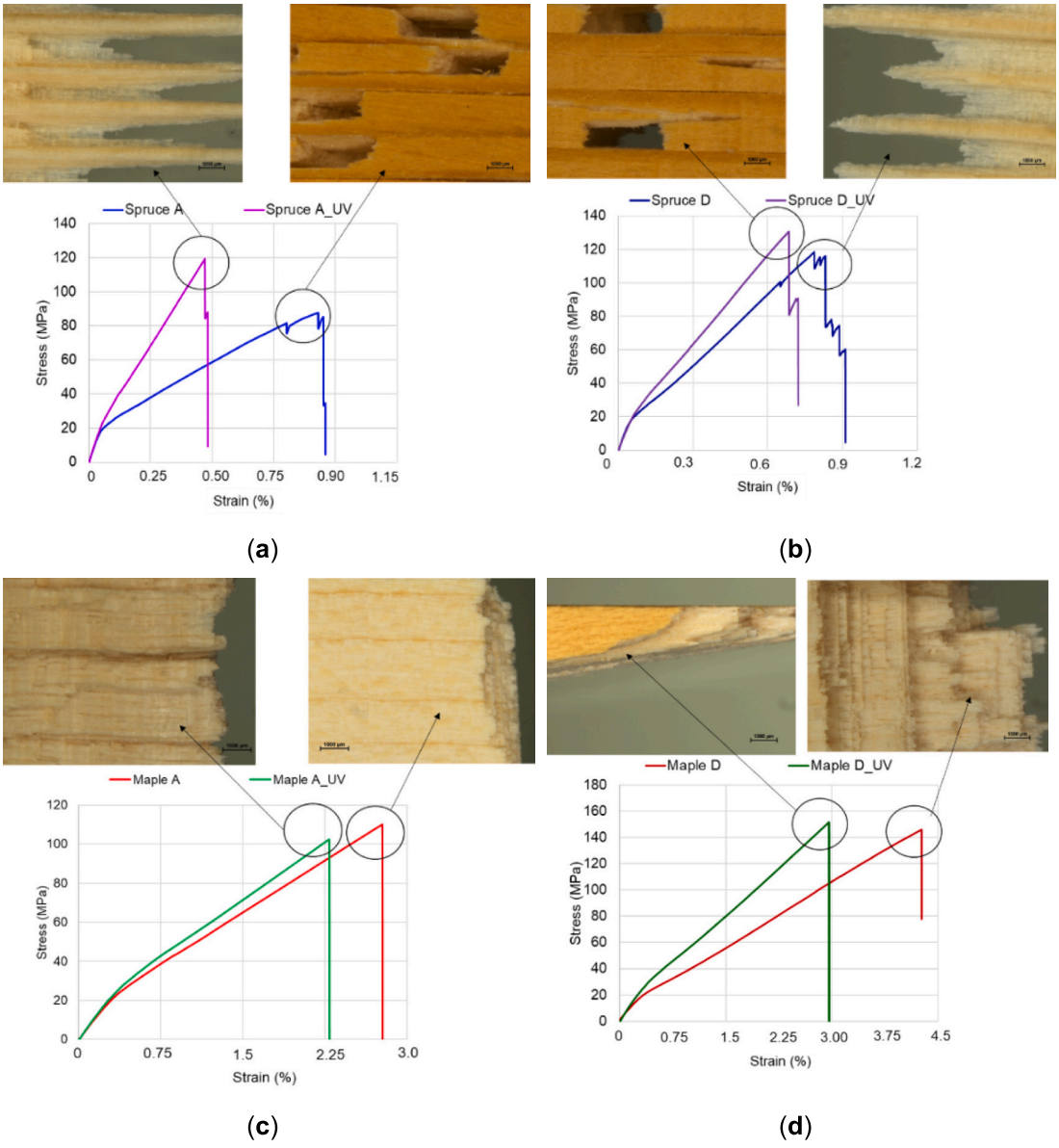

Fig. 4. Failure patterns obtained in destructive tests: (**a**) Spruce wood sample class A; (**b**) Spruce wood sample class D; (**c**) Maple wood sample class A; (**d**) Maple wood sample class D.

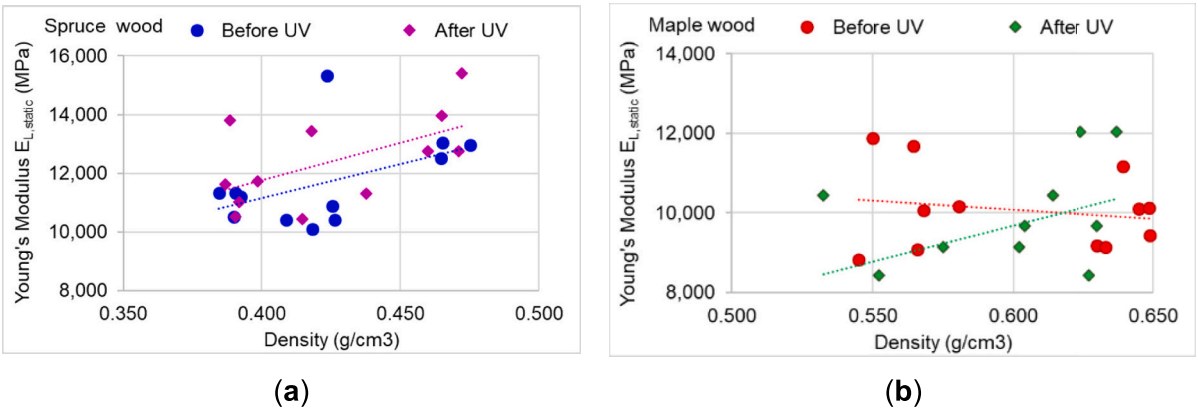

Fig. 5. Scatter plot $E_{L,static}$ over density for wood before and after 1000 h expose to artificial aging: (**a**) spruce wood samples; (**b**) maple wood sample.

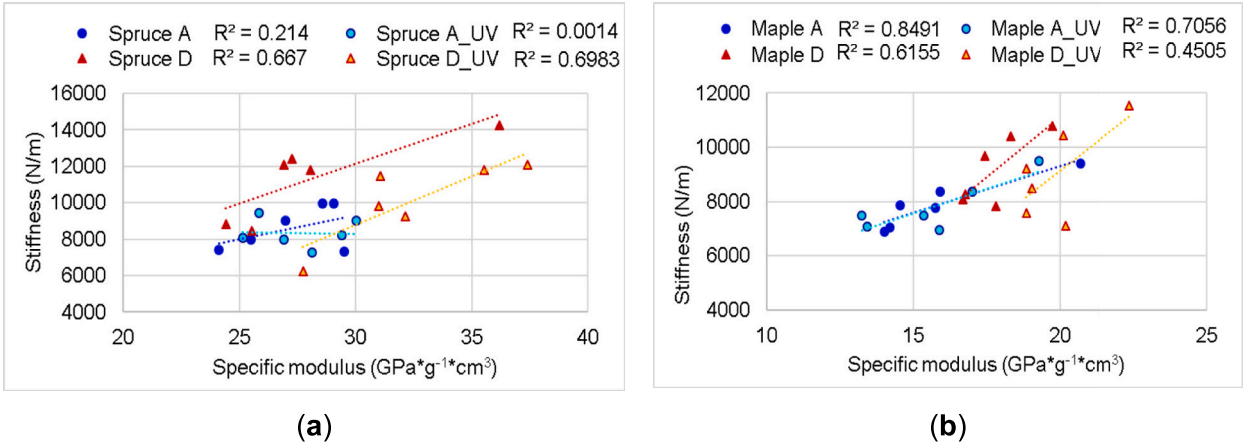

Fig. 6. Relationship between stiffness and specific modulus $(E_{L,static}/\rho)$ for wood before and after 1000 h exposure to artificial aging: (**a**) spruce wood samples; (**b**) maple wood sample.

Contrary to [43] who reports k_L values of 0.97 for spruce wood, in the current study, k_L is 1.098 for class A spruce, 1.142 for A_UV spruce and for D spruce; the value of the correction factor remains constant before and after aging, respectively the value of 1.065. In the case of maple wood samples, k_L is higher, being 1.185 (as an average value) for both unaged and aged samples. Although the simplified equation can be used for comparisons, it should be noted that differences in Poisson's ratios are not taken into account in this case, introducing uncertainty into the comparison, as mentioned by [33,35,36,43].

3.2. Changes in color properties

The color changes of the aged wood samples after the exposure for 1000 h can be observed with the naked eye, as highlighted in Fig. 8. Measuring the color parameters with specialized equipment and calculating the color difference based on eq. (6), showed that the color changes are more pronounced in spruce than in maple, and within each species, in spruce, class A more than class D, probably due to the higher lignin content. In the case of maple wood samples, the ratio is the reversed - samples from class D showed a more pronounced change in color compared to those from class A (Table 3). In terms of color intensity, the parameter C has the same value for spruce, regardless of the quality class, while for maple wood it varies, the color being more intense after artificial aging, especially for maple wood samples, class D maple. Wood exposed to direct sunlight undergoes chemical degradation caused by UV radiation.

According to [46,47], lignin contributes 80–95 %, carbohydrates 5–20 %, and extractives about 2 % to the total absorption coefficient of wood. Thus, lignin is the cell wall component most sensitive to UV light, it transfers UV light to the cellulose, which also leads to cellulose degradation according to the study described in [53]. In addition to photo-degradation, wood modification must also be considered, as the samples were also subjected to mild heating at a temperature of 50 °C, which may lead to the degradation of wood biopolymers. The more the wood changes its color in the direction of decreasing brightness, the more the surface temperature of the externally irradiated wood increases, reaching 60–90 °C, according to the research from [54,55]. Comparing the results obtained in this study with those highlighted by [56] who analyzed the color change of the samples after 600 h of exposure to artificial light, the recorded spruce wood ΔE^* is 19, and for the maple wood ΔE^* is 12; it was found that photodegradation for 1000 h led to ΔE^* varying between 23 and 25 for spruce wood, and ΔE^* varying between 14 and19 for maple wood, respectively. The color variation is mainly due to changes in the degree of yellow and red as a result of aging, visible in the magnitude of the difference in Chroma ΔC^*. The yellowing of wood samples after exposure to UV light reflects that they have undergone chemical changes as a consequence of the development of cromophoric compounds during lignin photodegradation [57–60].

3.3. Fourier transforms infrared spectroscopy (FTIR)

Due to their different structures of the two species, but also the way in which the anatomical elements are formed in the radial longitudinal section, the characteristic degradation processes, as well as their sensitivity to degradation, differ greatly. While photo-degradation of wood is

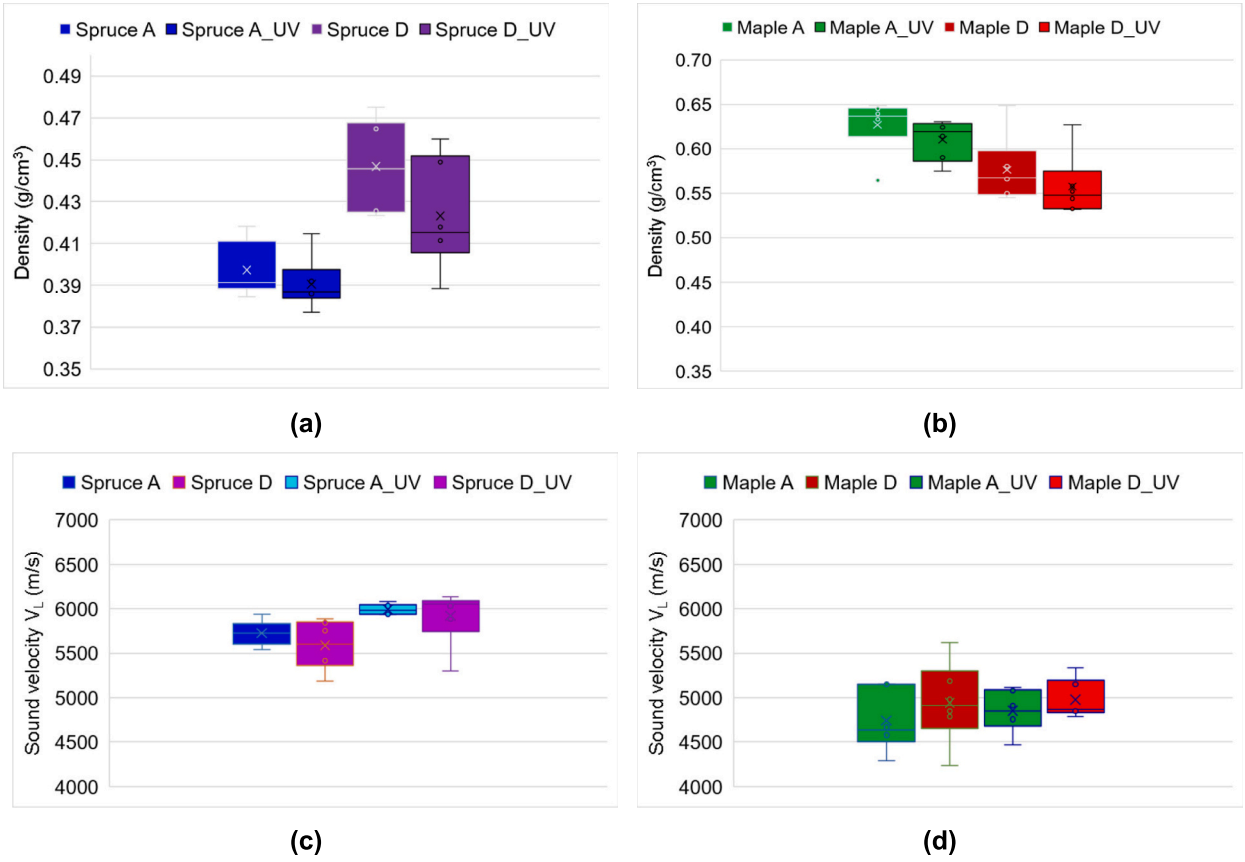

Fig. 7. Density variation of samples before and after aging in the case of spruce wood (**a**); Density variation of samples before and after aging in the case of maple wood (b); Sound velocity in longitudinal direction of spruce wood samples before and after aging (**c**); Sound velocity in longitudinal direction of maple wood samples before and after aging (**d**).

Table 2
Mean values and standard deviation of mechanical and acoustic properties of tested samples. Legend: MV – mean value; SD – standard deviation; ρ – density; $E_{L,dyn}$ – the dynamic elasticity modulus in longitudinal direction; $E_{L,static}$ – the modulus of elasticity in longitudinal direction obtained by static test; k_L – correction factor; $E^k_{L,dyn}/\rho$ – the specific modulus obtained from TOF test; $E^k_{L,static}/\rho$ – the specific modulus obtained by tensile test; S – the stiffness by tensile test; σ – tensile strength; ε - percentage strain at break.

Sample		ρ	$E_{L,dyn}$	$E_{L,static}$	k_L	$E^k_{L,dyn}/\rho$	$E_{L,static}/\rho$	S	σ	ε
		(kg/m^3)	(MPa)			(GPa*g^{-1}*cm^3)		(kN/m)	(MPa)	(%)
Spruce A	MV	397	13,031	10,822	1.098	33	27	8606	72	0.97
	SD	13	803	544	0.059	1.6	2.1	1206	24	0.77
Spruce A_UV	MV	391	14,480	11,102	1.142	35	28	8338	93	0.85
	SD	19	688	546	0.034	0.7	1.9	785	17	0.17
Spruce D	MV	447	14,006	12,519	1.060	31	28	11,304	105.	0.82
	SD	24	1747	1759	0.054	3.1	4.1	2238	15	0.35
Spruce D_UV	MV	423	14,918	13,687	1.071	35	32	10,112	106	0.77
	SD	35	2228	987	0.102	3.5	3.2	2220	15	0.05
Maple A	MV	627	14,091	9873	1.196	22	15	7888	86	1.28
	SD	31	1684	1028	0.076	3.2	2.5	930	25	0.73
Maple A_UV	MV	610	14,400	9587	1.230	23	15	7816	80	0.89
	SD	23	1544	1509	0.070	2.3	2.3	965	17	0.28
Maple D	MV	577	14,246	10,267	1.175	24	17	9170	116	2.07
	SD	38	3115	1088	0.126	4.5	1.1	1286	23	0.94
Maple D_UV	MV	558	13,887	10,109	1.116	24	18	9060	124	1.12
	SD	40	2130	2099	0.039	2.2	1.6	1694	24	0.34

considered a surface-related process due to limited penetration of light into wood [1,32,56], the mild heating on long-term exposure can affect the entire cross-section. Fig. 9 and Fig. 10 compare the FTIR spectra for spruce and maple samples, respectively, in the 2200–600 cm^{-1} footprint region.

3.3.1. FT-IR spectral analysis of spruce wood

Fig. 9 shows the FT-IR spectra for the spruce samples A and D after UV exposure, as well as for the control samples. The peak near 1730 cm^{-1} (non-conjugated carbonyl), corresponding to the C=O stretching vibration in the O-C=OH group of the glucuronic acid (GlcA) according to [61], shows an intensification in the treated samples as a result of

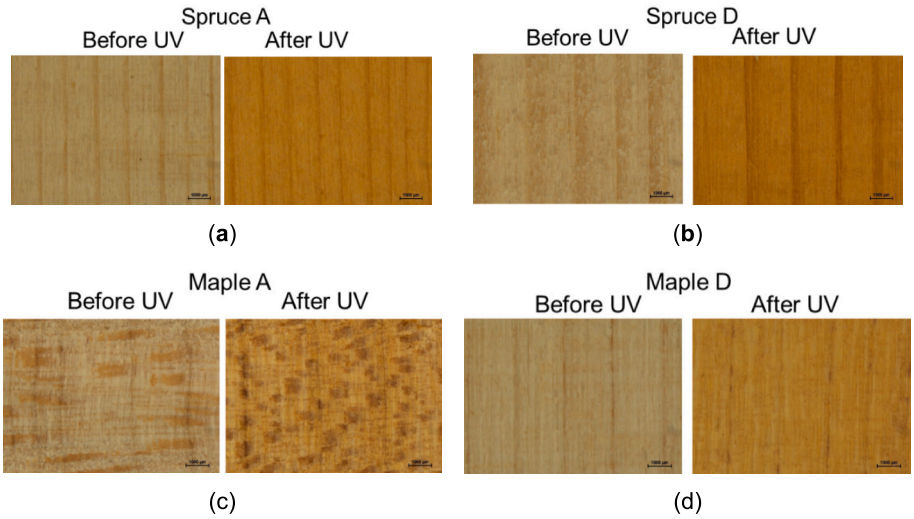

Fig. 8. Comparisons of the color of the samples before and after artificial aging: (**a**) Spruce wood sample class A; (**b**) Spruce wood sample class D; (**c**) Maple wood sample class A; (**d**) Maple wood sample class D.

Table 3
The mean values and SD for color parameters.

Sample		L*	a*	b*	E*	C*	ΔE^*	ΔC^*
Spruce A	MV	85.006	1.925	18.928	87.109	19.026	25.095	22.900
	SD	0.644	0.235	1.040	1.029	0.548		
Spruce A_UV	MV	74.736	7.526	41.130	85.638	41.813		
	SD	1.418	0.919	1.437	1.508	1.087		
Spruce D	MV	83.546	2.448	19.651	85.861	19.803	23.817	22.21
	SD	1.243	0.468	1.769	1.790	1.127		
Spruce D_UV	MV	74.941	7.312	41.320	85.890	41.962		
	SD	1.383	0.825	1.234	1.272	1.087		
Maple A	MV	78.973	4.280	16.937	80.882	17.469	13.801	12.97
	SD	4.161	1.035	0.851	1.023	3.924		
Maple A_UV	MV	74.254	5.612	29.838	80.221	30.361		
	SD	2.773	0.764	2.390	2.365	3.227		
Maple D	MV	84.968	2.410	16.513	86.591	16.687	18.866	16.04
	SD	1.836	0.636	0.669	0.713	1.721		
Maple D_UV	MV	75.043	5.514	32.254	81.867	32.722		
	SD	2.125	0.574	1.777	1.802	2.232		

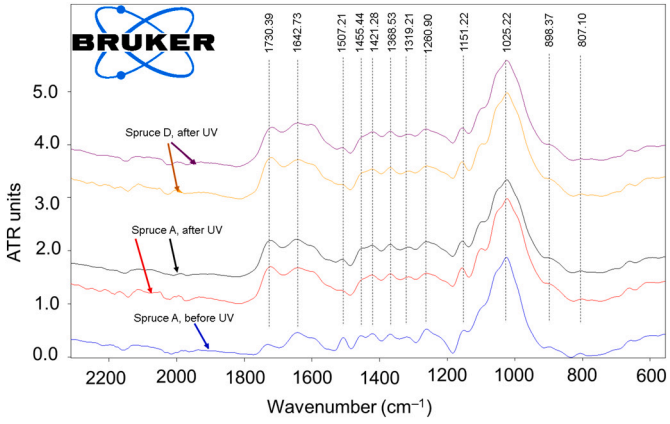

Fig. 9. Comparative FT-IR spectra for spruce wood before and after 1000 h of exposure to UV radiation.

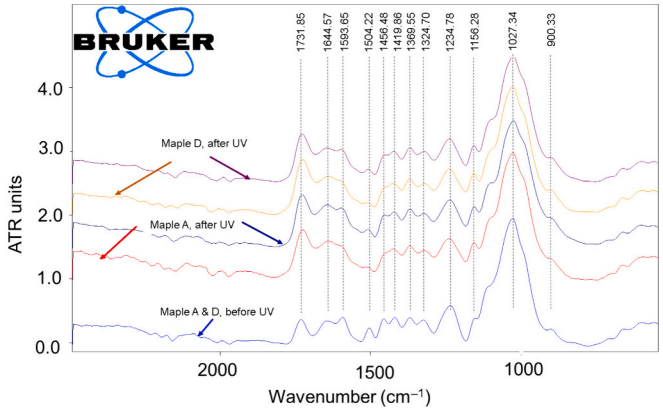

Fig. 10. Comparative FTIR spectra for maple wood samples before and after 1000 h of exposure to UV radiation.

some oxidation processes. The decrease of absorptions from 1507 cm^{-1} (vibration of the aromatic skeleton of lignin) is clearly observed. Analyzing the characteristic peaks of cellulose, the O—H bending vibration of water sorption at 1645 cm^{-1}, the C—H bending vibrations at 1370 cm^{-1} and the stretching vibration of the glucose ring at 1115 cm^{-1}, it was found that after UV exposure, the spruce wood shows an intensification of the absorptions from 1370 cm^{-1} and 1151 cm^{-1}, specific to the structural elements of prolisaccharides, correlating with the partial degradation of lignin. Lignin degradation after UV exposure of spruce

samples is evidenced by changes in the following bands: the aromatic skeletal vibration at 1507 cm^{-1}, the C—O stretching of the guaiacyl unit at 1260 cm^{-1} and the syringyl ring vibration, together with the C—O stretching at 1210 cm^{-1}. Similar results were reported by [61], for Chinese fir wood subjected to different heat treatment temperatures. An equally significant degradation is also observed for the 1455 cm^{-1} absorption band attributed to C—H deformation groups—lignin, carbohydrates: cellulose, hemicelluloses; CH2 bending—cellulose, according to [32,61–65].

3.3.2. FT- IR spectral analysis of maple wood

In the case of maple wood, the chemical degradation of the main chemical components of the wood is similar to that of spruce wood (Fig. 10). An interesting phenomenon in maple wood is the intensification of the absorption band at 1732 cm^{-1}, after exposure to UV radiation for 1000 h, which is characteristic to non-conjugated carbonyl groups. These changes highlight the degradation of lignin and the formation of chromophore compounds with carbonyl groups (aldehydes, ketones, acids and esters), results that are in good agreement with the specialized literature [32,62–66]. The absorption at 1645 cm^{-1} (conjugated carbonyl, aromatic ketones, quinones) remains clearly distinct and apparently slightly enhanced upon aging treatment (it may be associated with new chromophoric groups with conjugated carbonyl groups, including quinone-type structures). The decrease in absorptions attributed to lignin can be clearly seen from 1504 cm^{-1} (lignin aromatic skeleton vibration) and 1594 cm^{-1} (aromatic core). Thus, the absorption at 1594 cm^{-1} is no longer clearly distinct but becomes a shoulder in a wider band (approx. 1550–1700 cm^{-1}). The absorptions at 1370 cm^{-1} and 1156 cm^{-1} which are assigned to some structural elements of polysaccharides (cellulose, hemicelluloses) stand out better (intensification 1370 cm^{-1}, clear highlighting 1156 cm^{-1}) for aged samples and this observation can be correlated with the partial degradation of lignin.

According to [26,62–66], when cellulosic materials are exposed to an alternating wet-dry cycle, their mechanical flexibility and water accessibility are irreversibly reduced by the formation of irreversible intermolecular hydrogen bonds, which leads to the restriction of the mobility of amorphous carbohydrates. This phenomenon could explain both the increase in the rigidity of the wood and the speed of sound propagation in wood after aging. Similar studies have revealed that the most prone to photooxidation reactions is lignin, which decomposes approx. 80–95 % of UV light due to aromatic compounds, while cellulose and hemicellulose absorb only 5–20 % of UV light, according to [50,67–69]. The most significant peaks of the wood samples and their assignment in the FTIR spectra are shown in Table 4.

Table 4
Peaks of wood samples and their assignments in FTIR spectra.

Peak assignments	Compound	Wavenumber (cm^{-1})			
		Spruce		Maple	
		Before UV	After UV	Before UV	After UV
C=O stretching in ketone and carbonil groups	Hemicellulose	1730	1730↑	1732	1732↑
C=O stretching	Lignin	1642	1642↓	1645	1645↓
C=C stretching of the aromatic ring	Lignin	–	–	1594	1594↓
C=C stretching of the aromatic ring	Lignin	1507	1507↓	1504	1504↓
CH2 stretching	Lignin and hemicellulose	1455	1455↓	1456	1456↓
C–H bending	Cellulose and hemicellulose	1368	1368↑	1369	1369↑
C–H and O—H vibration	Polysaccharides (hemicellulose and hollocellulose)	1260	1260↓	1234	1234↓
C–O–C asymmetric stretching	Cellulose and hemicellulose	1151	1151↑	1156	1156↑
C–O stretching	Cellulose	1025	1025	1027	1027
C–H deformation	Cellulose	898	898↓	900	900↓

3.4. The crystallinity content

Wood crystallinity is defined as the weight fraction of crystalline cellulose. The increases in crystallinity affect the mechanical and acoustic properties, such as sound speed in the longitudinal direction, Young's modulus and stiffness increase, flexibility decreases with increasing crystallinity. Spruce wood shows a more homogeneous structure and reduced crystallinity dispersion depending on the quality class and specific modulus, unlike maple wood which is characterized by a higher anisotropy, less crystalline cellulose content before aging artificial but with greater sensitivity to the aging treatment. As can be seen from Fig. 11, the crystal diffraction peaks appear near 17° and 22.5° of the X-ray diffraction angle (2θ) which represents the crystal diffraction intensity of wood cellulose as reported in [70–73]. The diffraction patterns obtained on samples before and after UV exposure differ considerably both from one species to another and from one anatomical structure organization to another (class A spruce and maple, and class D spruce and maple, respectively).

The diffraction patterns obtained on the samples before and after UV exposure differ considerably from one species to another as well as from one anatomical structure organization to another (class A spruce and maple, and class D spruce and maple, respectively). This is caused by the differences in the crystallinity of the samples, determined both by the proportion of early wood - late wood, the width of the annual rings, the regularity of the annual rings, the degree of fiber waviness (in the case of maple samples), the age of the tree/annual ring and not in the last row of angle microfibrils that reflect different crystallinity [72]. It is observed that the class A spruce and class D maple samples show an increase in crystallinity after exposure to UV radiation, compared to the other categories (class D spruce and class A maple) where the crystallinity decreases after UV exposure. The crystallinity index for class D spruce wood is 17 % lower after UV exposure, and for class A spruce wood, the crystallinity index increases by 2.8 %. The largest increases are for D class maple wood, with the crystallinity index being 17 % higher after exposure. For class A maple wood, the crystallinity index decreases by 2.8 %. Similar values regarding the crystallinity index for common spruce wood were also reported in [70–73]. Over 900 h of wood aging, the crystalline structure underwent negative changes with a decrease in the percentage of crystallinity determined mainly by cellulose depolymerization after long UV aging. The crystallinity of spruce wood is higher than that of maple wood by approx. 30 % as can be seen in Fig. 12, comparing the crystallinity before the applied treatment.

4. Conclusions

This study is a multiscale analysis of the effect of artificial wood aging for musical instruments through physical, mechanical, acoustic and chemical measurements of spruce and maple wood samples. The paper demonstrated that artificial aging for 1000 h of exposure leads to chemical changes with more effect on sound speed than mechanical properties. Thus, the parameters most affected by artificial aging were the speed of sound propagation, which was significantly higher in the class A spruce wood samples and the longitudinal modulus of elasticity in the class A maple wood samples. These results are correlated with the increase in the crystallinity index. An improvement in acoustic and mechanical properties after UV exposure was noticed for maple class D, where both stiffness and crystallinity index increased. The results highlighted the heterogeneous nature of wood, even within the same

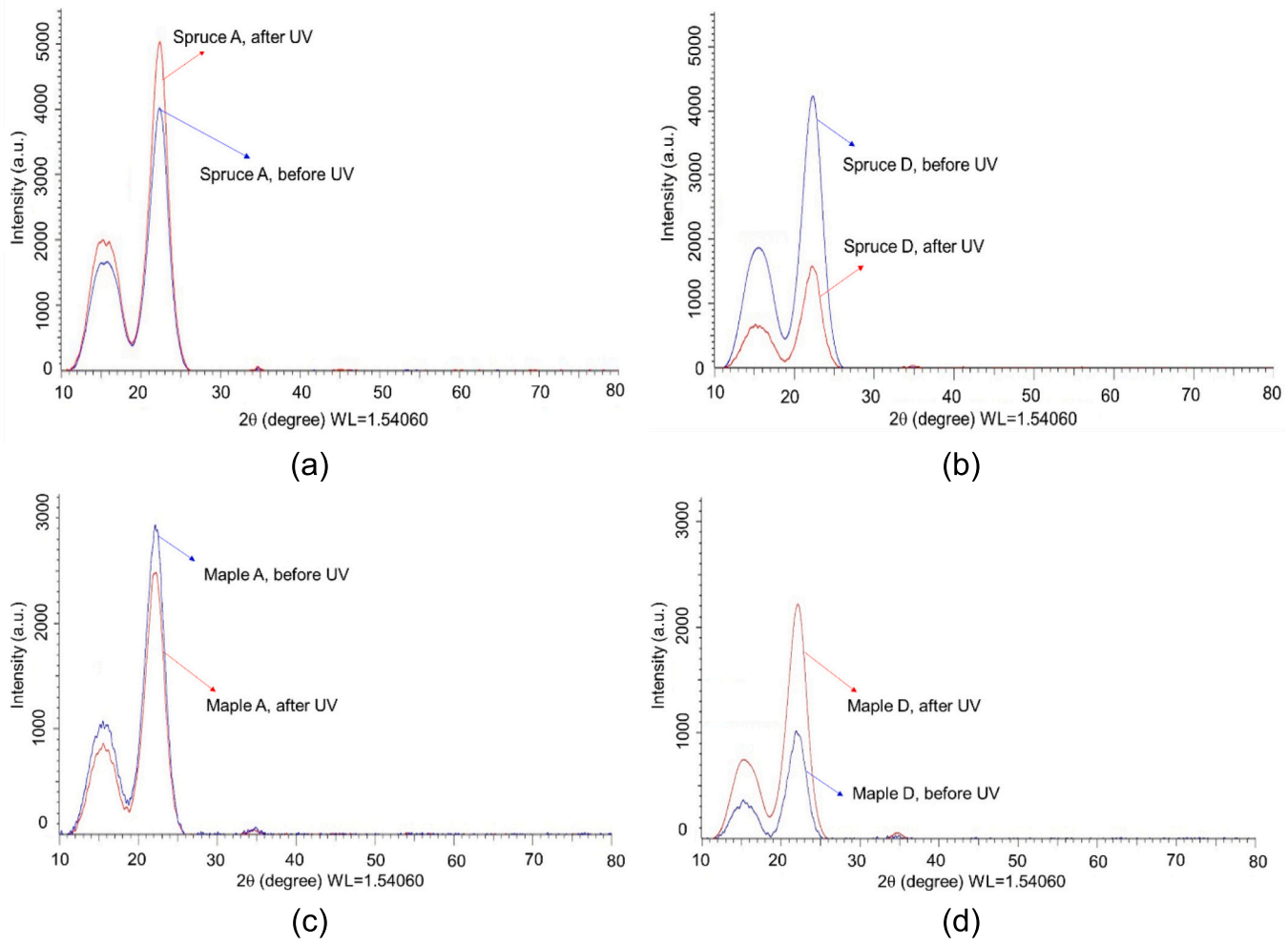

Fig. 11. XRD patterns of the control and aged wood: a) spruce wood grade A; b) spruce wood grade D; c) maple wood grade A; d) maple wood grade D.

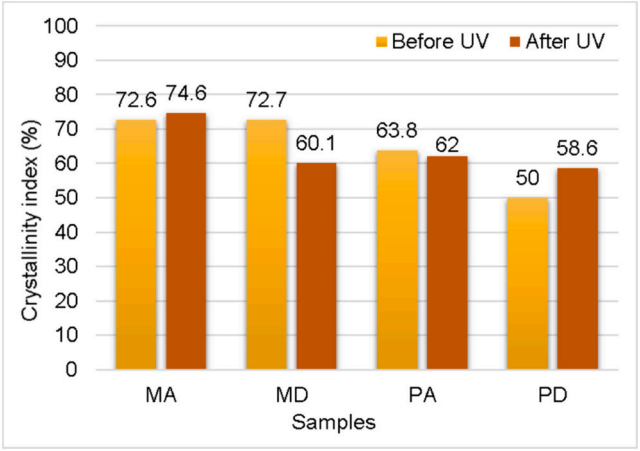

Fig. 12. Crystallinity index comparisons.

species, where the proportion of early wood - late wood, the amount of polysaccharides and the anatomical architecture of the wood lead to different chemical, acoustic and mechanical changes, under the same conditions of UV irradiation.

The physical and chemical changes produced by artificial aging, manifested by the breaking of covalent bonds in organic polymers, the reduction of mass, the increase of surface roughness, the increase of hydrophobicity and stability to humidity variations, the decrease of the lignin content in the soundboard can lead to the improvement of the acoustic properties (speed of sound propagation and acoustic radiation) of the wood used in musical instruments. Applying a light photo-degradation treatment, before assembling the plates in the violin body, could result in an increase in the acoustic performance of the instrument, similar to old, naturally aged instruments.

CRediT authorship contribution statement

Mariana Domnica Stanciu: Writing – original draft, Software, Resources, Project administration, Investigation, Funding acquisition, Formal analysis, Conceptualization. **Horatiu Draghicescu Teodorescu:** Software, Methodology, Investigation, Formal analysis, Data curation. **Sorin Vlase:** Writing – review & editing, Supervision, Methodology, Investigation. **Mircea Mihalcica:** Writing – original draft, Visualization, Validation, Data curation, Conceptualization. **Mihaela Cosnită:** Writing – original draft, Software, Methodology, Formal analysis, Data curation. **Adriana Savin:** Writing – review & editing, Validation, Data curation, Conceptualization.

Declaration of competing interest

The authors declare that they have no known competing financial interests or personal relationships that could have appeared to influence the work reported in this paper.

Data availability

Data will be made available on request.

Acknowledgments

This research was supported by a grant from the Ministry of Research, Innovation and Digitization, CNCS/CCCDI—UEFISCDI, project number 61PCE/2022, PN-III-P4-PCE2021-0885, ACADIA—Qualitative, dynamic and acoustic analysis of anisotropic systems with modified interfaces. The authors acknowledge the structural funds project PRO-DD (POS-CCE, O.2.2.1., ID 123, SMIS 2637, No. 11/2009) for providing the infrastructure used in this research. We are grateful to the technical staff of Gliga Musical Instruments, Reghin, a Romanian manufacturer of musical string instruments, for supplying the specimens. We would like to thank Prof. Timar Cristina from the Transilvania University of Brasov for the support given in carrying out the FTIR analyses.

References

[1] Y. Kataoka, M. Kiguchi, R.S. Williams, P.D. Evans, Violet light causes photodegradation of wood beyond the zone affected by ultraviolet radiation, Holzforschung 61 (1) (2007) 23–27.
[2] E.A. Salca, T. Krystofiak, B. Lis, S., Hiziroglu glossiness evaluation of coated wood surfaces as function of varnish type and exposure to different conditions, Coatings 11 (2021) 558.
[3] B.F. Tjeerdsma, M. Boonstra, A. Pizzi, P. Tekely, H. Militz, Characterisation of thermally modified wood: molecular reasons for wood performance improvement, Holz Roh Werkst. 56 (3) (1998) 149–153.
[4] M.D. Stanciu, M. Mihălcică, F. Dinulică, A.M. Nauncef, R. Purdoiu, R. Lăcătuș, G. V. Gliga, X-ray imaging and computed tomography for the identification of geometry and construction elements in the structure of old violins, Materials 14 (2021) 5926.
[5] B.C. Stoel, T.M. Borman, A comparison of wood density between classical Cremonese and modern violins, PLoS One 3 (7) (2008) e2554.
[6] N. Sodini, D. Dreossi, R. Chen, M. Fioravanti, Non-invasive microstructural analysis of bowed stringed instruments with synchrotron radiation X-ray microtomography, J. Cult. Herit. 13 (2012) 44–49.
[7] A.S. Srndovic, Interactions between Wood Polymers in Wood Cell Walls and Cellulose/Hemicellulose Biocomposites, Thesis for The Degree Of Doctor Of Philosophy, Department of Chemical and Biological Engineering, Chalmers University of Technology, Göteborg, Sweden, 2011 (accessed on 28.08.2023).
[8] N. Španić, V. Jambreković, M. Klarić, Basic chemical composition of wood as a parameter in raw material selection for biocomposite production, Cellul. Chem. Technol. 52 (3–4) (2018) 163–169.
[9] M. Cosnita, C. Cazan, M.A. Pop, D. Cristea, Aging resistance under short time ultraviolet (UV) radiations of polymer wood composites entirely based on wastes, Environ. Technol. Innov. 31 (2023). Article 103208.
[10] F.F.P. Kollmann, A. Wilfred, J. Côté, Principles of Wood Science and Technology I, Springer-Verlag, New York Inc., New York, 1968, pp. 1–54.
[11] D. Fengel, Ultrastructural behaviour of cell wall polysaccharides, TAPPI J. 53 (3) (1970) 497–503.
[12] A.J. Kerr, D.A.I. Goring, The ultrastructural arrangement of the wood cell wall, Cellul. Chem. Technol. 9 (6) (1975) 563–573.
[13] K.L. Kato, R.E. Cameron, A review of the relationship between thermally-accelerated ageing of paper and hornification, Cellulose 6 (1999) 23–40.
[14] H.T. Chang, T.F. Yeh, S.T. Chang, Comparisons of chemical characteristic variations for photodegraded softwood and hardwood with/without polyurethane clear coatings, Polym. Degrad. Stab. 77 (1) (2002) 129–135.
[15] T.C. Chang, H.T. Chang, C.L. Wu, S.T. Chang, Influences of extractives on the photodegradation of wood, Polym. Degrad. Stab. 95 (2010) 516–521.
[16] S.A. Sebnem, D.T. Eylem, A.E. Mahmut, I. Yildirim, Natural weathering of sixteen wood species: changes on surface properties, Polym. Degrad. Stab. 183 (2021) 109415.
[17] S. Yildiz, E.D. Gezer, U.C. Yildiz, Mechanical and chemical behavior of spruce wood modified by heat, Build. Environ. 41 (12) (2006) 1762–1766.
[18] C. Gomri, M. Cretin, M. Semsarilar, Recent progress on chemical modification of cellulose nanocrystal (CNC) and its application in nanocomposite films and membranes-a comprehensive review, Carbohydr. Polym. 294 (2022) (Article 119790).
[19] P. Niemz, T. Hofmann, T. Rétfalvi, Investigation of chemical changes in the structure of thermally modified wood, Maderas-Ciencia Y Tecnologia 12 (2) (2010) 69–78.
[20] J. Bourgois, G. Janin, R. Guyonnet, The color measurement - a fast method to study and to optimize the chemical-transformations under - gone in the thermically treated wood, Holzforschung 45 (5) (1991) 377–382.
[21] M. Hakkou, M. Petrissans, P. Gerardin, A., Zoulalian investigations of the reasons for fungal durability of heat-treated beech wood, Polym. Degrad. Stab. 91 (2) (2006) 393–397.
[22] J.J. Weiland, R. Guyonnet, Study of chemical modifications and fungi degradation of thermally modified wood using DRIFT spectroscopy, Holz Roh Werkst. 61 (3) (2003) 216–220.
[23] K. Kránitz, *Effect of natural aging on wood*. PhD Thesis ETH Zurich (2014), accessed on 01.08.2023.
[24] N. Zeniya, E. Obataya, K. Endo-Ujiie, M. Matsuo-Ueda, Changes in vibrational properties and colour of spruce wood by hygrothermally accelerated aging at 95–140 °C and different relative humidity levels, SN. Appl. Sci. 1 (2019) 7.
[25] M. Yokoyama, J. Gril, M. Matsuo, H. Yano, et al., Mechanical characteristics of aged Hinoki (*Chamaecyparis obtusa* Endl.) wood from Japanese historical buildings, in: International Conference on Wooden Cultural Heritage, Evaluation of Deterioration and Management of Change, 2009, 8p ffhal-00795997.
[26] T. Noguchi, E. Obataya, K. Ando, Effects of aging on the vibrational properties of wood, J. Cult. Herit. 13 (3) (2012) 21–25.
[27] K. Kránitz, M. Deublein, P. Niemz, Determination of dynamic elastic moduli and shear moduli of aged wood by means of ultrasonic devices, Mater. Struct. 47 (6) (2014) 925–936.
[28] C.K. Su, S.Y. Chen, J.H. Chung, G.C. Li, B. Brandmair, et al., Materials engineering of violin soundboards by Stradivari and Guarneri, Angew. Chem. Int. Ed. Eng. 60 (35) (2021) 19144–19154, https://doi.org/10.1002/anie.202105252 (Epub 2021 Jun 27. PMID: 34062043; PMCID: PMC8457145).
[29] W.C. Feist, D.N.-S. Hon, Chemistry of weathering and protection, in: R. Rowell (Ed.), The Chemistry of Solid Wood, Advances in Chemistry Series, vol. 207, American Chemical Society (ACS), Washington DC, 1984, pp. 401–454.
[30] F. Dinulică, M.D. Stanciu, A. Savin, Correlation between anatomical grading and acoustic–elastic properties of resonant spruce wood used for musical instruments, Forests 12 (2021) 1122.
[31] F. Dinulică, A. Savin, M.D. Stanciu, Physical and acoustical properties of wavy grain sycamore maple (Acer pseudoplatanus L.) used for musical instruments, Forests 14 (2023) (Article 197).
[32] L. Gurău, M.C. Timar, C. Coșereanu, M. Cosnita, M.D. Stanciu, Aging of wood for musical instruments: analysis of changes in color, surface morphology, chemical, and physical-acoustical properties during UV and thermal exposure, Polymers 15 (2023) (Article 1794).
[33] M.K. Andrews, Which acoustic speed?, in: Proceedings of the 13th International Symposium on Non-destructive Testing of Wood, University of California, Berkeley Campus California, USA, 19–21, August, 2002.
[34] M.K. Andrews, Wood quality measurement, *Son et Lumiere*, N. Z. J. For. 47 (2002) 19–21.
[35] M. Legg, S. Bradley, Measurement of stiffness of standing trees and felled logs using acoustics: a review, J. Acoust. Soc. Am. 139 (2) (2016) 588–604.
[36] H. Hansen, Acoustic Studies on Wood, Master Thesis, University of Canterbury New Zealand, 2006. accessed on 20 August 2023.
[37] R. Gall, M.D. Stanciu, E. Filimon, M. Cosnita, V.G. Gliga, The influence of artificial aging on resonance wood on its physical characteristics, in: Proceedings of the 9th International Conference on Advanced Composite Materials Engineering, 2022, pp. 73–81.
[38] M.D. Stanciu, H.D. Teodorescu, S. Vlase, Degradation of mechanical properties of pine wood under symmetric axial cyclic loading parallel to grain, Polymers 12 (2020) 2176.
[39] M.D. Stanciu, H.D. Teodorescu, I.C. Roșca, Mechanical properties of GFRPs exposed to tensile, compression and tensile–tensile cyclic tests, Polymers 13 (2021) 898.
[40] V. Bucur, R.R. Archer, Elastic constants for wood by an ultrasonic method, Wood Sci. Technol. 18 (4) (1984) 255–265.
[41] V. Bucur, Acoustics of Wood, 2nd ed, Springer, Berlin, Germany, 2006, pp. 173–196.
[42] R. Gonçalves, A.J. Trinca, Comparison of elastic constants of wood determined by ultrasonic wave propagation and static compression testing, Wood Fiber Sci. 43 (1) (2011) 64–75.
[43] P. Niemz, D. Caduff, Research into determination of the Poisson ratio of spruce wood, Holz Roh Werkst. 66 (1) (2008) 1–4.
[44] M.D. Stanciu, D. Sova, A. Savin, N. Ilias, G.A. Gorbacheva, Physical and mechanical properties of ammonia-treated black locust wood, Polymers 12 (2020) 377.
[45] P. Bekhta, T. Krystofiak, B. Lis, N. Bekhta, The impact of sanding and thermal compression of wood, varnish type and artificial aging in indoor conditions on the varnished surface color, Forests 13 (2022) 300.
[46] H. Norrstrom, Light absorbing properties of pulp and pulp components. 1. Method, Svensk Papperstidning-Nordisk Cellulosa 72 (*2*) (1969) 25–31.
[47] M.L. Kuo, N.H. Hu, Ultrastructural changes of photodegradation of wood surfaces exposed to UV, Holzforschung 45 (5) (1991) 347–353.
[48] J. Keckes, I. Burgert, K. Frühmann, M. Müller, K. Kölln, et al., Cell-wall recovery after irreversible deformation of wood, Nat. Mater. 2 (2003) 810–814.
[49] C.M. Altaner, M.C. Jarvis, Modelling polymer interactions of the 'molecular Velcro' type in wood under mechanical stress, J. Theor. Biol. 253 (2008) 434–445.
[50] M.F. Ashby, K.E. Easterling, R. Harrysson, S.K. Maiti, The fracture and toughness of woods, Proc. R. Soc. London, Ser. A 398 (1985) 261–280.
[51] C. Lanvermann, P. Hass, F.K. Wittel, P. Niemz, Mechanical properties of Norway spruce: intra-ring variation and generic behavior of earlywood and latewood until failure, Bioresources 9 (2014) 105–119.
[52] A.L. Christoforo, T.H. Panzera, F.A.R. Lahr, Estimation of tensile strength parallel to grain of wood species, Engenharia Agrícola 39 (4) (2019) 533–536.
[53] M.N. Yildirim, B. Uysal, A. Ozcifci, A.H. Ertas, Determination of fatigue and static strength of scots pine and beech wood, Wood Research 60 (4) (2015) 679–686.
[54] T. Yoshimoto, Photochemical analysis of wood and related sunstances, J Japan *Wood Res Soc.* 18 (1) (1972) 45–49.

[55] L. Tolvaj, S. Molnár, Photodegradation and thermal degradation of outdoor wood, in: Joseph Gril (Ed.), Wood Science for Conservation of Cultural Heritage –Braga 2008: Proceedings of the International Conference Held by COST Action IE0601 (Braga - Portugal, 5–7 November), 2008, pp. 67–72.
[56] U. Müller, M. Rätzsch, M. Schwanninger, M. Steiner, H. Zobl, Yellowing and IR-changes of spruce wood as result of UV-irradiation, J. Photochem. Photobiol. B Biol. 69 (2003) 97–105.
[57] L. Oltean, A. Teischinger, C. Hausmann, Wood surface discolouration due to simulated indoor sunlight exposure, Holz Roh Werkst. 66 (1) (2008) 51–56.
[58] H. Wikberg, S.L. Maunu, Characterisation of thermally modified hard- and softwoods by C-13 CPMAS NMR, Carbohydr. Polym. 58 (4) (2004) 461–466.
[59] J. Geffertová, A. Geffert, E. Výbohová, The effect of UV irradiation on the colour change of the spruce wood, Acta Facultatis Xylologiae Zvolen 60 (1) (2018) 41–50.
[60] E. Karami, I. Brémaud, S. Bardet, T. Almeras, D. Guibal, P. Langbour, K. Pourtahmas, J. Gril, Reversible and irreversible effects of mild thermal treatment on the properties of wood used for making musical instruments: comparing mulberry to spruce, iForest 15 (2022) 256–264, https://doi.org/10.3832/ifor4074-015.
[61] S. Cheng, A. Huang, S. Wang, Q. Zhang, Effect of different heat treatment temperatures on the chemical composition and structure of Chinese fir wood, BioRes 11 (2) (2016) 4006–4016.
[62] M.C. Timar, A.M. Varodi, L. Gurau, Comparative study of photodegradation of six wood species after short-time UV exposure, Wood Sci. Technol. 50 (2016) 135–163.
[63] X.Y. Liu, M.C. Timar, A.M. Varodi, An investigation of accelerated temperature-induced aging of four wood species: colour and FTIR, Wood Sci. Technol. 51 (2017) 357–378.
[64] X.Y. Liu, M.C. Timar, A.M. Varodi, R. Nedelcu, M. Torcătoru, Colour and surface chemistry changes of wood surfaces coated with two types of waxes after seven years exposure to natural light in indoor conditions, Coatings 12 (2022) 1689.
[65] C. Boeriu, D. Bravo, R. Gosselink, J. Dam, Characterisation of structure-dependent functional properties of lignin with infrared spectroscopy, Ind. Crop. Prod. 20 (2004) 205–218.
[66] R. Javier-Astete, J. Melo, J. Jimenez-Davalos, et al., Classification of Amazonian fast-growing tree species and wood chemical determination by FTIR and multivariate analysis (PLS-DA, PLS), Sci. Rep. 13 (2023) 7827, https://doi.org/10.1038/s41598-023-35107-6.
[67] K. Kránitz, W. Sonderegger, C.T. Bues, P. Niemz, Effects of aging on wood: a literature review, Wood Sci. Technol. 50 (1) (2016) 7–22.
[68] M. Báder, R. Németh, J. Sandak, et al., FTIR analysis of chemical changes in wood induced by steaming and longitudinal compression, Cellulose 27 (2020) 6811–6829.
[69] D. Wang, L. Lin, F. Fu, et al., The fracture mechanism of softwood via hierarchical modelling analysis, J. Wood Sci. 65 (58) (2019) 1–11.
[70] R.S. Davidson, The photodegradation of some naturally occurring polymers, J. Photochem. Photobiol. B Biol. 33 (1996) 3–25.
[71] F. Lionetto, R. Del Sole, D. Cannoletta, G. Vasapollo, A. Maffezzoli, Monitoring wood degradation during weathering by cellulose crystallinity, Materials 5 (2012) 1910–1922.
[72] S. Andersson, R. Serimaa, T. Paakkari, P. Saranpää, E. Pesonen, Crystallinity of wood and the size of cellulose crystallites in Norway spruce (Picea abies), J. Wood Sci. 49 (2003) 531–537.
[73] A. Cogulet, P. Blanchet, V. Landry, Wood degradation under UV irradiation: A lignin characterization, J. Photochem. Photobiol. B Biol. 158 (2016) 184–191.